Diyala Journal for Pure Science

Density Distributions of Exotic ^{17}F and ^{19}C Nuclei Studied by the Two-Body Model

Alzahraa Yaseen A. Alsajjad and Ahmed N. Abdullah*

Department of Physics – College of Science – University of Baghdad – Baghdad – Iraq

* Ahmednajim@scbaghdad.edu.iq

Received: 16 May 2019 **Accepted: 16 July 2019**

DOI: https://dx.doi.org/10.24237/djps.15.04.511B

Abstract

The two-body model of $[Core + p(n)]$ within the single-particle wave functions of the Woods-Saxon (WS) and Harmonic Oscillator (HO) potentials has been used to study the ground state features such as the neutron, proton and matter densities, the associated root mean square (rms) radii and elastic form factors of exotic ^{17}F and ^{19}C nuclei. The long tail manner is clearly shown in the calculated matter densities of these nuclei. According to the calculated results it is found that this model provides a good description on the nuclear structure of above exotic nuclei. The reaction cross sections for these nuclei have been studied using the Glauber model with an optical limit approximation at high energy region.

Keywords: Exotic nuclei, Two-body model, Glauber model, Woods-Saxon potential.

دراسة توزيعات الكثافة للنوى الغريبة ^{17}F و ^{19}C باستخدام أنموذج الجسيمين

الزهراء ياسين عبدالسجاد و أحمد نجم عبدالله

قسم الفيزياء – كلية العلوم – جامعة بغداد – بغداد – العراق

Diyala Journal for Pure Science

Density Distributions of Exotic ^{17}F and ^{19}C Nuclei Studied by the Two-Body Model

Alzahraa Yaseen A. Alsajjad and Ahmed N. Abdullah

الخلاصة

تم استخدام أنموذج الجسيمين مع الدوال الموجية للجسيمة المفردة لجهدي وودز- ساكسون والمتذبذب التوافقي لدراسة خصائص الحالة الارضية مثل توزيعات الكثافة النيوترونية، البروتونية والكتلية وانصاف الاقطار النووية وعوامل التشكل للنوى الغريبة ^{17}F و^{19}C . خاصية الامتداد الطويل تم الحصول عليها في توزيعات الكثافة الكتلية لهذه النوى. وفقا للنتائج المحسوبة وجد ان هذا الانموذج يعطي وصفاً جيدا للتركيب النووي لنوى الهالة تحت الدراسة. المقاطع العرضية للتفاعل تمت دراستها باستخدام نموذج جلوبر عند الطاقات العالية.

الكلمات المفتاحية: النوى الغريبة، انموذج الجسيمين، نموذج جلوبر، جهد وودز- ساكسون.

Introduction

The study of the structure of exotic (halo) nuclei near the proton and neutron drip lines has become a hot topic in nowadays nuclear physics due to their exotic features [1-3]. The halo phenomena occur mainly due to the small separation energy of the last few nucleons and their occupation on the states with low angular momentum (l = 0, 1) [4] which allow the wave function of halo (valence) nucleons to extend to large matter radii [5].

Both on experiments and theories, studying the halo structure is very important to understand the nucleus structure. The halo nuclei must be studied by radioactive beam facilities because they are so short-lived [6].

The few body models can be used to describe halo systems, where the halo nuclei are assumed to be formed by coupling a compact core surrounded by a few weakly bound nucleons [7].

Therefore, we can divide halo systems into two main types: the two-body system where the core nucleus is surrounded by one valence nucleon, such as the one proton halo ^{12}N and the one neutron halo ^{15}C; and the three-body system where the core nucleus is surrounded by two valence (halo) nucleons, such as ^{11}Li and ^{14}Be. The three-body system is called Borromean because the two-body subsystems (core plus one nucleon or the di-nucleon) are unbound, while the three-body system is bounded [8].

Hamoudi *et al.* [9] have used the TFSM and the BCM to study the ground state densities of exotic ^{9}C, ^{12}N and ^{23}Al nuclei. The long tail property is shown in the calculated proton and matter densities of these nuclei. The calculated results of matter densities were in good accordance with the experimental results.

Abdullah [10] has used a three-body model of (Core + *n* + *n*) to study the ground state densities of halo ^{6}He, ^{11}Li, ^{12}Be and ^{14}Be nuclei. The long tail property is shown in the calculated neutron and matter densities of these nuclei. The calculated results of matter densities were in good accordance with the experimental results.

In the present work, the two-body model of $[Core + p(n)]$ will be used within the single-particle wave functions of the Woods-Saxon (WS) and Harmonic Oscillator (HO) potentials to study the ground state features such as the neutron, proton and matter densities, the associated root mean square (rms) radii and elastic form factors of exotic ^{17}F and ^{19}C nuclei. The reaction cross sections for these nuclei will be studied using the Glauber model with an optical limit approximation at high energy region.

Theory

For exotic (halo) nuclei the matter density can be written as [11]:

$$\rho_m(r) = \rho_c(r) + \rho_v(r) \tag{1}$$

Where $\rho_c(r)$ and $\rho_v(r)$ are the core density and valence (halo) density, respectively.

In this work, the ground state densities of exotic (halo) nuclei have been calculated via two methods, these are WS+WS (Woods-Saxon) and HO+HO (Harmonic Oscillator).

In the WS+WS method, the densities for the core and valence nucleon (proton or neutron) are calculated by solving the eigenvalue problem of Woods-Saxon potential [12]:

$$\frac{\hbar^2}{2m}\frac{d^2R_{nlj}(r)}{dr^2} + \left[\varepsilon_{nlj} - V(r) - \frac{\hbar^2}{2m}\frac{l(l+1)}{r^2}\right]R_{nlj}(r) = 0 \tag{2}$$

Where m is the reduced mass of the core and single nucleon, ε_{nlj} is the single-particle energy, $R_{nlj}(r)$ is the radial eigen function of WS potential and $V(r)$ is the potential of the core and can be written as [12]:

$$V(r) = V_0(r) + V_{so}(r)\,\vec{l}.\vec{s} + V_c(r) \tag{3}$$

Where $V_0(r)$ is the spin-independent central potential:

$$V_0(r) = \frac{-V_0}{1+\left[e^{(r-R_0)/a_0}\right]} \tag{4}$$

$V_{so}(r)$ is the spin-orbit potential:

$$V_{so}(r) = V_{so}\frac{1}{r}\left[\frac{d}{dr}\frac{1}{1+\left(e^{(r-R_{so})/a_{so}}\right)}\right] \tag{5}$$

and $V_c(r)$ is the Coulomb potential generated by a homogeneous charged sphere of radius R_c [13]:

$$V_c(r) = \frac{Ze^2}{r} \qquad \text{for} \quad r \geq R_c \tag{6}$$

$$V_c(r) = \frac{Ze^2}{R_c}\left[\frac{3}{2} - \frac{r^2}{2R_c^2}\right] \qquad \text{for} \quad r < R_c \tag{7}$$

The radii R_0,R_{so} and $R_c$are usually expressed as [10]:

$$R_i = r_i\,A^{1/3} \tag{8}$$

Where A is the nuclear mass number

In the HO + HO method, the densities for the core and valence nucleon are given by the harmonic oscillator wave functions [11, 14]:

$$\rho_c(r) = \frac{1}{4\pi}\sum_{n\ell} X_c^{n\ell}\,|R_{n\ell}(r)|^2 \tag{9}$$

$$\rho_v(r) = \frac{1}{4\pi} X_v^{n\ell} |R_{n\ell}(r)|^2 \quad (10)$$

Where $X_{c(v)}^{n\ell}$ represents the number of neutrons or protons, in the sub-shell nlj.
The matter density of Eq. (1) can be written as [10]:

$$\rho_m(r) = \rho^n(r) + \rho^p(r) \quad (11)$$

Where $\rho^n(r)$ and $\rho^p(r)$ are the neutron and proton densities, respectively which can be written as [10]:

$$\rho^n(r) = \rho_c^n(r) + \rho_v^n(r) \quad (12)$$

$$\rho^p(r) = \rho_c^p(r) + \rho_v^p(r) \quad (13)$$

The rms radii of the neutron and proton distributions can be calculated by [10]:

$$r_g = \langle r_g^2 \rangle^{1/2} = \left[\frac{\int r^2 \rho_g(r) dr}{\int \rho_g(r) dr}\right]^{1/2} \qquad g = n, p \quad (14)$$

We study the elastic form factors for considered nuclei using the Plane Wave Born Approximation (PWBA) within the proton density distribution $\rho_p(r)$. In the PWBA, the elastic form factors are written as [15]:

$$F(q) = \frac{4\pi}{Z} \int_0^\infty \rho_p(r) j_0(qr) r^2 dr \quad (15)$$

Where $j_0(qr)$ is the zero-order spherical Bessel function and q is the momentum transfer from the incident electron to the target nucleus. Inclusion the corrections of the finite nucleon size $F_{fs}(q) = exp\,(-0.43q^2/4)$ and the center of mass $F_{cm}(q) = exp(b^2q^2/4A)$ in the calculations (when HO wave function is used) needs multiplying the form factors of Eq. 15by these corrections.

The reaction cross section of considered nuclei is studied by the Glauber model within Optical Limit (OL) approximation which can be expressed as [16]:

$$\sigma_R = 2\pi \int [1 - T(b)]\, b\, db \left(1 - \frac{B_c}{E_{cm}}\right) \quad (16)$$

Where E_{cm} is the kinetic energy in the center of mass system, B_c is Coulomb barrier and $T(b)$ is the transparency function at impact parameter b.

In OL approximation the $T(b)$ is written as

$$T(b) = \left|S_{el}^{OL}(b)\right|^2 \quad (17)$$

Where $S_{el}^{OL}(b)$ is the elastic $S-$matrix for the target-projectile system given as [17]:

$$S_{el}^{OL}(b) = exp[iO_{PT}(b)] \quad (18)$$

$$O_{PT}(b) = \int_{-\infty}^{\infty} dR_3 \int d\vec{r}_1 \int d\vec{r}_2 \rho_P(r_1)\rho_T(r_2) f_{NN}(|\vec{R} + \vec{r}_1 - \vec{r}_2|) \quad (19)$$

is the overlap of the ground state densities of projectile and target ($\rho_P$and ρ_T, respectively)

Results and Discussion

The two-body model of $[Core + p(n)]$ has been used within the single-particle wave functions of the WS and HO potentials to study the ground state features such as the proton, neutron and matter densities, the associated root mean square (rms) radii and elastic form factors of exotic ^{17}F and ^{19}C nuclei. The reaction cross sections for these nuclei have been studied using the Glauber model with an Optical Limit (OL) approximation at high energy region. A structure of a core ^{16}O [^{18}C] plus valence one proton [neutron] is assumed for ^{17}F [^{19}C].

The configurations $\{(1s_{1/2})^4, (1p_{3/2})^8, (1p_{1/2})^4\}$ and $\{(1s_{1/2})^4, (1p_{3/2})^8, (1p_{1/2})^2, (1d_{5/2})^4\}$ are considered for core ^{16}O and ^{18}C nuclei, respectively.

The valence (halo) proton of ^{17}F is considered as admixture between $1d_{5/2}$ and $2s_{1/2}$ with occupation probabilities of 0.4 and 0.6, respectively, the mixing configuration of the valence proton is assumed as following [18]:

$$\phi = \left\{\sqrt{\alpha}\,\phi_{2s_{1/2}} + \sqrt{1-\alpha}\,\phi_{1d_{5/2}}\right\}$$

Where α refer to the occupation probability of the ($2s_{1/2}$) orbital. While the valence neutron of ^{19}C is assumed to be in a pure $2s_{1/2}$. Table 1 exhibits some features [19 and 20] of halo ^{17}F and ^{19}C nuclei.

The WS parameters for stable nuclei (^{19}F and ^{12}C) and the depth of WS potential (V_0) for core nucleons of halo nuclei ^{17}F and ^{19}C are taken from Ref. [21] whereas the V_0 for valence nucleon (proton or neutron) and other parameters (*i.e.* V_{so}, r_0, r_{so}, a_0, a_{so} and r_c) are adjusted to reproduce the experimental single particle energy of a valence nucleon and matter rms radii.

The HO size parameters b_c and b_v are adjusted to reproduce the experimental rms matter radii for core (^{16}O, ^{18}C) and halo nuclei (^{17}F, ^{19}C), respectively.

The HO size parameter (b_c, b_v) and WS parameters utilized in our calculations are tabulated in table 2. In tables 3 and 4 a comparison is made between the obtained and experimental results [22-24] of the neutron, proton, core and matter rms radii in fermis for ^{17}F and ^{19}C halo nuclei along with the calculated results of Refs. [13 and 22] for ^{17}F and Refs. [25 and 26] for ^{19}C. Within errors the obtained results are consistent with experimental ones more than those of above Refs.

Table 5 displays the obtained results of the single-particle energies (ε) for the above investigated nuclei.

Table 1: Some properties of nuclei under study

Halo nucleus	J^π [19]	Type of halo nucleus	Half-life time $(\tau_{1/2})$ [19]	Separation Energy (MeV) [20]
^{17}F	$5/2^+$	One proton halo	$64.37\ s$	$S_p = 0.6$
^{19}C	$1/2^+$	One neutron halo	$46.2\ ms$	$S_n = 0.58$

Table 2: The HO size parameter WS parameters utilized in our calculations

Nuclei	V_0 (MeV)		V_{so} (MeV)	$a_0 = a_{so}$ (fm)	$r_0 = r_{so}$ (fm)	r_c (fm)	b (fm)	
	Core	Valence					b_c	b_v
^{17}F	53.692	48.66 for $1d_{5/2}$ 51.93 for $2s_{1/2}$	6.0	0.585	1.253	1.406	1.695	2.80
^{19}C	50.187	37.570	6.0	0.572	1.318	1.393	1.81	3.72
^{19}F	52.842		6.0	0.618	1.352	1.492	1.712	
^{12}C	62.512		6.0	0.735	1.392	1.457	1.572	

Table 3: Calculated and experimental results of the neutron and proton rms radii

Nuclei	$\langle r_n^2\rangle^{1/2}$ (fm)		$\langle r_n^2\rangle_{exp}^{1/2}$ (fm) [22]	$\langle r_n^2\rangle_{th.}^{1/2}$ (fm) [22,25]	$\langle r_p^2\rangle^{1/2}$ (fm)		$\langle r_p^2\rangle_{exp}^{1/2}$ (fm) [22,23]	$\langle r_p^2\rangle_{th.}^{1/2}$ (fm) [22,25]
	HO	WS			HO	WS		
^{17}F	2.54	2.56	2.48±0.18	2.53	2.96	2.85	2.9±0.15	2.74
^{19}C	3.43	3.36	----	3.37	2.66	2.63	2.4±0.03	2.38

Table 4: Calculated and experimental results of the core and matter rms radii

Nuclei	$\langle r_c^2\rangle^{1/2}$ (fm)		$\langle r_c^2\rangle_{exp}^{1/2}$ (fm) [24]	$\langle r_c^2\rangle_{th.}^{1/2}$ (fm) [13, 26]	$\langle r_m^2\rangle^{1/2}$ (fm)		$\langle r_m^2\rangle_{exp}^{1/2}$ fm) [22,24]	$\langle r_m^2\rangle_{th.}^{1/2}$ (fm) [13,25]
	HO	WS			HO	WS		
^{17}F	2.54	2.58	2.54±0.02	2.65	2.77	2.71	2.71 ± 0.18	2.74
^{19}C	2.86	2.83	2.82±0.04	2.82	3.21	3.15	3.23 ± 0.08	3.09

Table 5: The calculated single-particle energies

Nucleus	nl_j	*neutron*	*proton*
		ε_{cal} (MeV)	ε_{cal} (MeV)
^{17}F	$1s_{1/2}$	34.336	30.114
	$1p_{3/2}$	20.555	16.631
	$1p_{1/2}$	17.184	13.255
	$1d_{5/2}$	----	0.6
	$2s_{1/2}$	----	0.6
^{19}C	$1s_{1/2}$	33.543	30.967
	$1p_{3/2}$	21.083	18.698
	$1p_{1/2}$	18.154	----
	$1d_{5/2}$	8.237	----
	$2s_{1/2}$	0.58	----

Figure 1 demonstrates the calculated matter densities for ^{17}F (top panel) and ^{19}C (bottom panel) calculated via WS+ WS figures (1a and 1c) and HO+ HO figures (1b and 1d) methods.

Therein, the blue, red and dashed distributions correspond to core, halo and matter densities, respectively, whereas the shaded areas refer to the experimental matter densities of ^{17}F [22] and ^{19}C [27]. The obtained results give a good description of the experimental data and show a characteristic behavior for a halo structure (*i.e.* long tail manner) component in the matter densities.

Figure 2 exhibits the neutron, proton and matter densities displayed as blue, red and dashed curves, respectively. From figures (2a, 2b, 2c and 2d) it is obvious that the proton [neutron] densities have a long tail with respect to the neutron [proton] densities, this means that ^{17}F [^{19}C] is proton [neutron] halo nucleus.

A comparison of the theoretical matter densities of unstable ^{17}F and ^{19}C halo nuclei (dashed curves) with those of their stable isotopes ^{19}F and ^{12}C (red curves) are presented in figures (3a and 3d). As shown from these figures, the dashed and red curves are quite diverse. As the valence proton [neutron] in ^{17}F [^{19}C] is loosely bound, the dashed curves have a longer tail than those of the red curves.

Figure 4 exemplifies the theoretical form factors for ^{19,17}F figures (4a and 4b) and ^{12,19}C figures (4c and 4d) calculated using PWBA within proton densities obtained by WS+ WS (left panel) and HO + HO (right panel) methods.

Therein, the red and blue curves correspond to C0 of unstable (^{17}F, ^{19}C) and stable (^{19}F, ^{12}C) nuclei, respectively. For comparison the experimental data of stable ^{19}F [28] and ^{12}C [29] are plotted by blue-dotted symbols. According to these results, each of the red and blue curves has only one diffraction minimum. The minima location of ^{17}F [^{19}C] has outward and downward [inward and upward] shift as compared with the minima of ^{19}F [^{12}C].

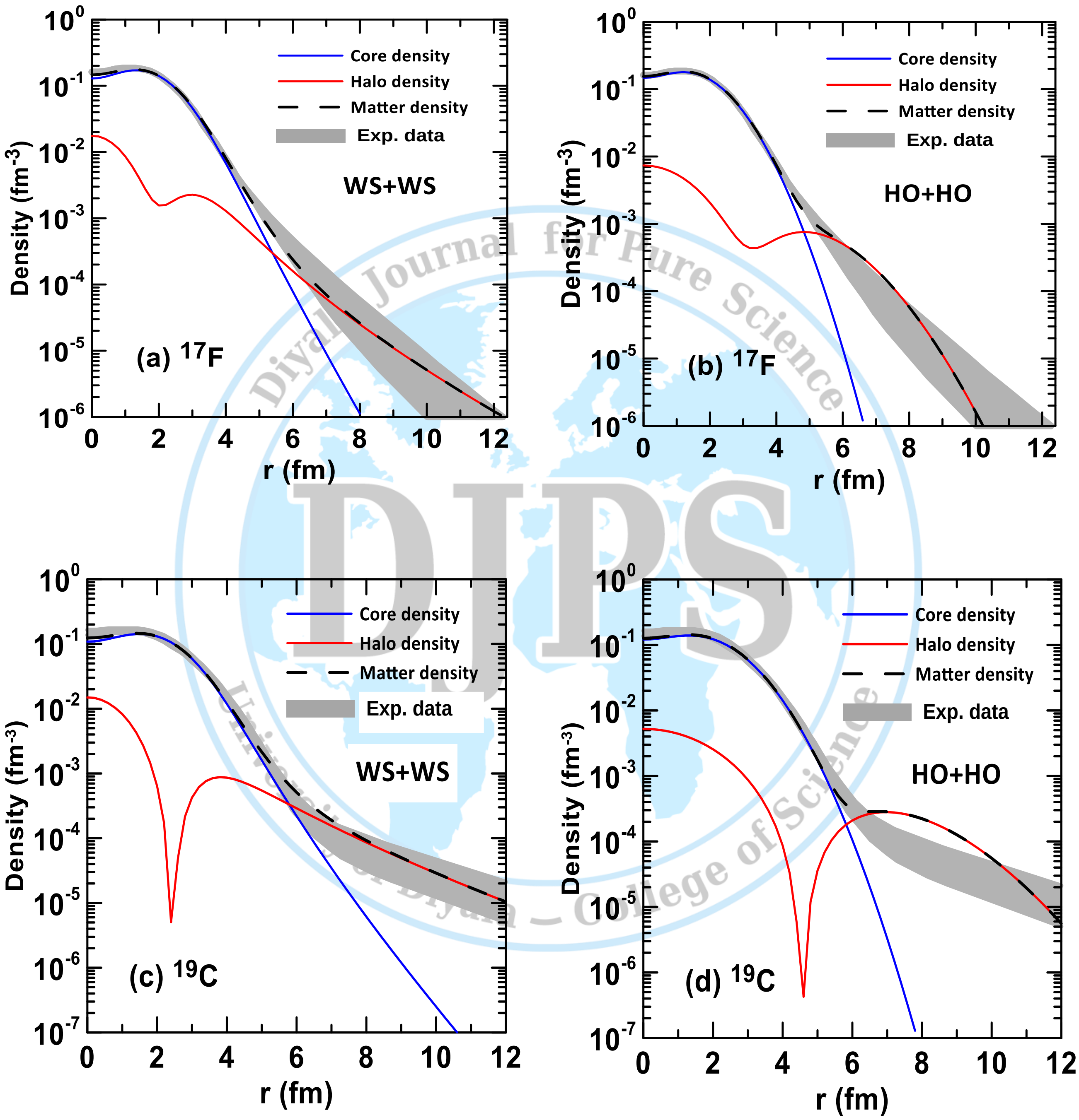

Figure 1: The core, valence and matter densities for halo ^{17}F and ^{19}C nuclei.

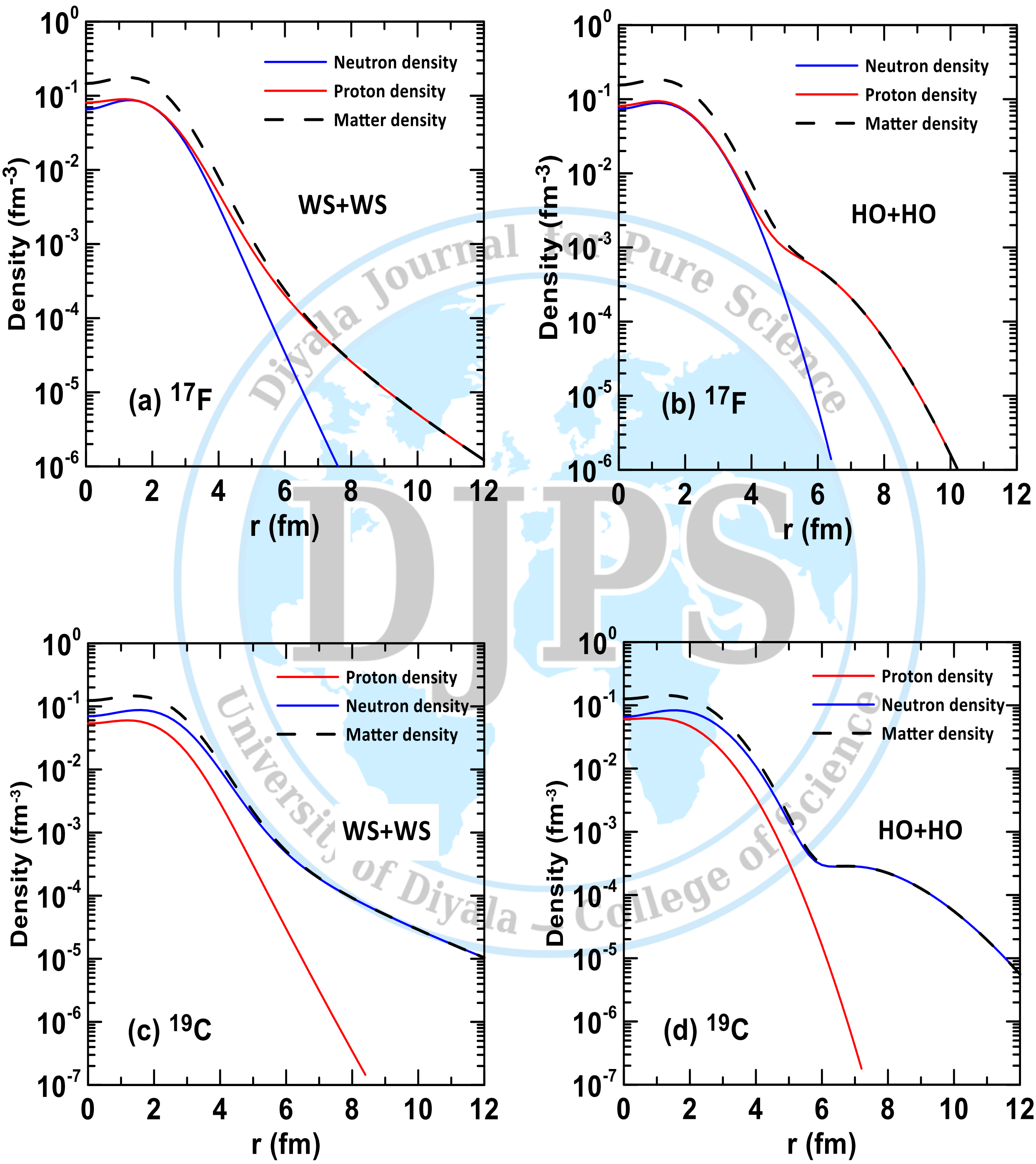

Figure 2: Distributions of the neutron, proton and matter densities for halo ^{17}F and ^{19}C nuclei.

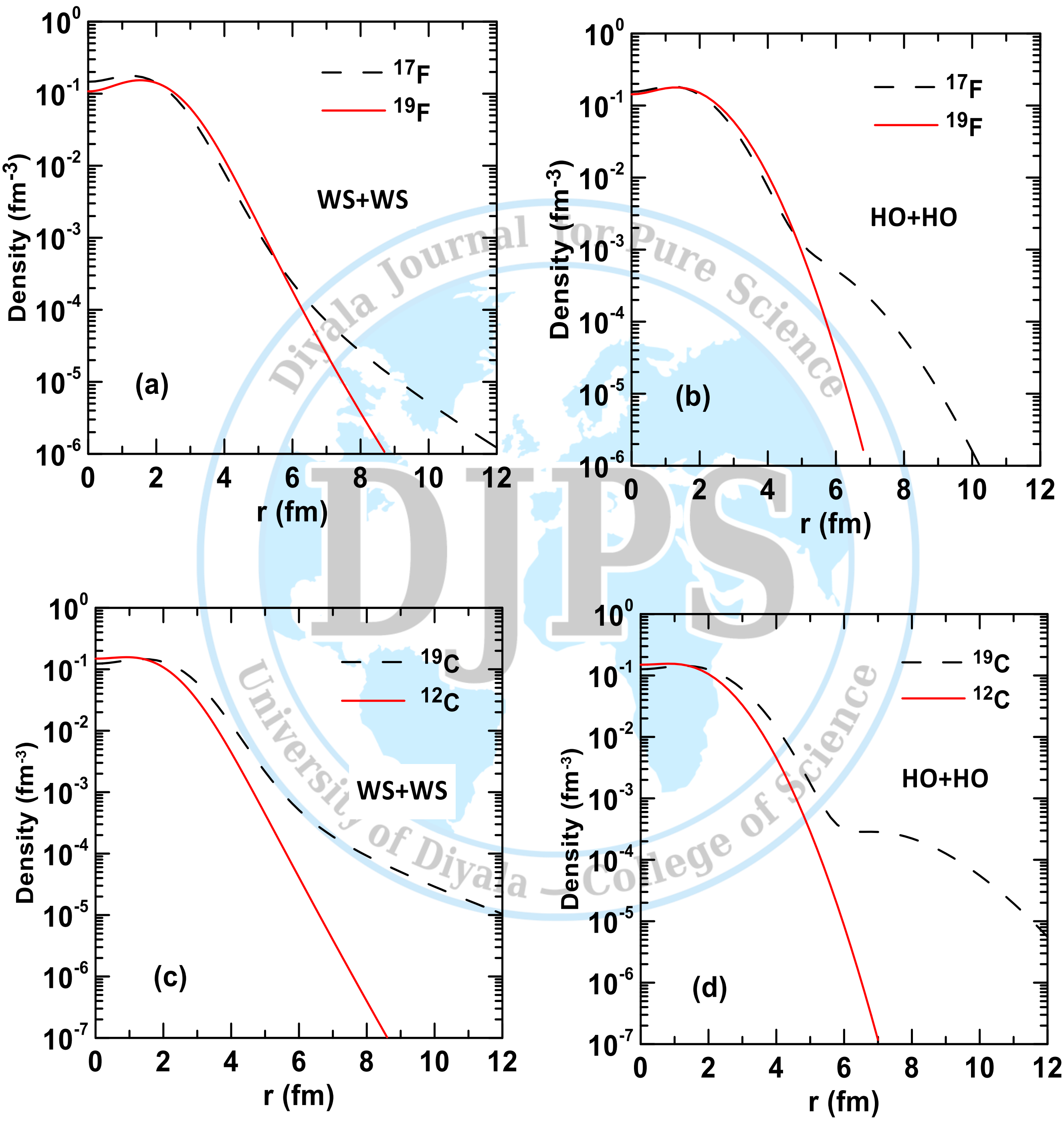

Figure 3: Distributions of the matter density for unstable (^{17}F,^{19}C) nuclei and their stable isotopes (^{19}F,^{12}C)

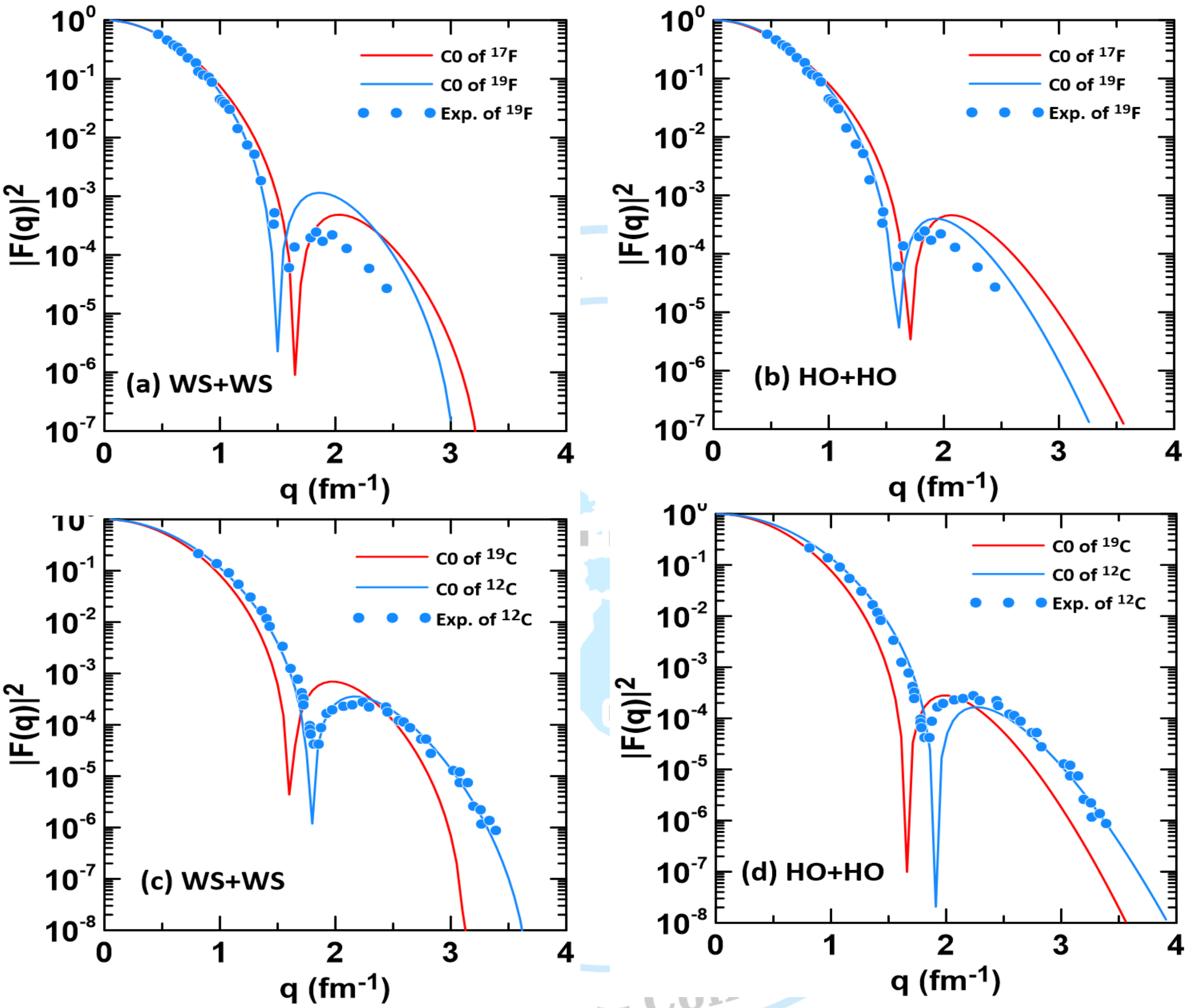

Figure 4: Elastic form factors of unstable (^{17}F,^{19}C) nuclei and their stable isotopes (^{19}F,^{12}C)

The reaction cross sections (σ_R) of ^{17}F and ^{19}C on ^{12}C target have been calculated using the Glauber model with an optical limit approximation at high energy region and tabulated in table 6 along with experimental data [24]. From this table one can see that the calculated results of σ_R are in a good agreement with experimental data.

Diyala Journal for Pure Science

Table 6: Calculated reaction cross sections of ^{17}F and ^{19}C along with experimental data.

Halo nuclei	Calculated σ_R (mb)	Experimental σ_R (mb) [24]	Energy (MeV) [24]
^{17}F	789	982 ± 32	650
	970	966 ± 56	700
^{19}C	1240	1231 ± 28	960

Conclusions

According to the calculated results it is found that the two-body model of $[Core + p(n)]$ within the single-particle wave functions of the WS and HO potentials provides a good description on the nuclear structure of exotic ^{17}F and ^{19}C nuclei. The long tail manner is clearly shown in the matter densities of these nuclei. The structure of the halo (valence) proton in ^{17}F is a mixed configuration of $1d_{5/2}$ and $2s_{1/2}$ with dominant $2s_{1/2}$ whereas the structure of the halo (valence) neutron in ^{19}C is in a pure $2s_{1/2}$. The calculated results of σ_R using the Glauber model with an optical limit approximation at high energy region are in a good agreement with experimental data.

References

1. Tanihata, H. Savajols, R. Kanungo, Progress in Particle and Nuclear Physics, 68, pp. 215(2013).

2. G. A. Korolev, A.V. Dobrovolsky, A.G. Inglessi, G.D. Alkhazov, P. Egelhof, A. Estradé, I. Dillmann, F. Farinon, H. Geissel, S. Ilieva, Y. Ke, Physics Letters, B 780, pp. 200(2018).

3. A. V. Dobrovolsky, G. A. Korolev, A. G. Inglessi, G. D. Alkhazov, G. Colò, I. Dillmann, P. Egelhof, A. Estradé, F. Farinon, H. Geissel, S. Ilieva, Nuclear Physics,A 989 , pp. 40 (2019).

4. W. Zaijun, Z. Z. Ren, Science in China Series G Physics and Astronomy, 47, pp. 42 (2004).

5. B. Blank, C. Marchand, M.S. Pravikoff, T. Baumann, F. Boué, H. Geissel, M. Hellström, N. Iwasa, W. Schwab, K. Sümmerer, M. Gai, Nuclear Physics, A 624, pp. 242 (1997).

6. A. N. Antonov, D. N. Kadrev, M.K. Gaidarov, E.M. De Guerra, P. Sarriguren, J.M. Udias, V.K. Lukyanov, E. V. Zemlyanaya, G.Z. Krumova, Physical Review,C 72, pp.044307-1 (2005).
7. G. Wen-Jun, J. Huan-Qing, L. Jian-Ye, Z.Wei, R. Zhong-Zhou, L. Xi-Guo, Communications in Theoretical Physics, 40(5), pp. 577 (2003)
8. H. Z.Guo, W. Meng, X. HuShan, S. ZhiYu, W. JianSong, X. GuoQing, Z. WenLong, X. ZhiGang, M. RuiShi, L. Chen, Z. XueYing, Z. HongBin, Z. TieCheng, X. ZhiGuo, W. Yue, C. RuoFu, H. TianHeng, F. Fen, G. Qi, H. JianLong, Z. XueHeng, Z. Chuan, Y. YuHong, G. ZhongYan, Science in China Series G: Physics, Mechanics and Astronomy ,51(7), pp.781-787 (2008).
9. A. K. Hamoudi, G. N. Flaiyh, A. N. Abdullah, Iraqi Journal of Science, 56 (1A), pp. 147-161 (2015).
10. A. N. Abdullah, International Journal of Modern Physics E, 26 ,1750048 (2017).
11. A. N. Abdullah, Indian Journal of Natural Sciences ,8 ,13898(2018).
12. B. A. Brown, S. E. Massent, P. E. Hodgson, journal of Physics G: Nuclear Physics, 5(12) pp.1655(1979).
13. Y. Chu, Z. Z. Ren, C. Xu, The European Physical Journal A, 37(3), pp.361-366 (2008).
14. A. P. J Brussard, P. W. M. Glademans, Shell-model Application in Nuclear Spectroscopy, (North-Holland Publishing Company, Amsterdam.1977).
15. A. N. ANTONOV, M. K. GAIDAROV, D. N. KADREV, P. E. HODGSON, E. MOYA DE GUERRA, International Journal of Modern Physics E, 13(4), pp. 759-772 (2004).
16. T. Zheng, T. Yamaguchi, A. Ozawa, M. Chiba, R. Kanungo, T. Kato, K. Katori, K. Morimoto, T. Ohnishi, T. Suda, I. Tanihata, Y. Yamaguchi, A.Yoshida, K. Yoshida, H. Toki, N. Nakajima, Nuclear Physics A, 709(1-4), pp.103-118(2002).
17. J. A. Tostevin, J. S. Al-Khalili, Nuclear Physics A ,616, 418c (1997).
18. F. De-Qing, M. Chun-Wang, M. Yu-Gang, C. Xiang-Zhou, C. Jin-Gen, C. Jin-Hui, G. Wei, T. Wen-Dong, W. Kun, W. Yi-Bin, Y. Ting-Zhi, Z. Chen, Z. Jia-Xu, S. Wen-Qing, Chinese Physics Letters, 22(3) ,pp. 572-575(2005).

19. G. Audi, F.G. Kondev, M. Wang, W. J. Huang, S. Naimi, Chinese Physics C, 41 (3) 030001-1(2017).

20. M. Wang, G. Audi, F.G. Kondev, W.J. Huang, S. Naimi, X. Xu, Chinese Physics C ,41 (3), 030003-1(2017).

21. B. A. Brown, W. D. M. Rae, Nushell@MSU, MSU-NSCL report (2007).

22. H.Y. Zhang, W. Q. Shen, Z. Z. Ren, Y. G. Ma, W. Z. Jiang, Z. Y. Zhu, X. Z. Cai, D. Q. Fang, C. Zhong, L. P. Yu, Y. B. Wei, W. L. Zhan, Z. Y. Guo, G. Q. Xiao, J. S. Wang, J. C. Wang, Q. J. Wang, J. X. Li, M. Wang, Z. Q. Chen, Nuclear Physics A ,707 ,pp. 303–324(2002).

23. R. Kanungo, W. Horiuchi, G. Hagen, G. R. Jansen, P. Navratil, F. Ameil, J. Atkinson, Y. Ayyad, D.Cortina-Gil, I. Dillmann, A. Estrad´, A. Evdokimov, F. Farinon, H. Geissel, G. Guastalla, R.Janik, M. Kimura, R. Kn¨obel, J. Kurcewicz, Yu. A. Litvinov, M. Marta, M. Mostazo, I. Mukha, C. Nociforo, H.J. Ong, S. Pietri, A. Prochazka, C. Scheidenberger, B. Sitar, P. Strmen, Y. Suzuki, M. Takechi, J. Tanaka, I. Tanihata, S. Terashima, J. Vargas, H. Weick, J. S. Winfield ,Physical Review Letters ,117 ,102501 (2016).

24. A. Ozawa, T. Suzuki, I. Tanihata, Nuclear Physics A, 693, pp. 32-62(2001).

25. B. Abu-Ibrahim, W. Horiuchi, A. Kohama, and Y. Suzuki, Physical Review C ,77, 034607 (2008).

26. H.T. Fortune, R. Sherr, The European Physical Journal A, 47 (154), (2011).

27. A. Ozawa, The European Physical Journal A-Hadrons and Nuclei, 13 (1-2), pp. 163(2002).

28. P. L. Hallowell, W. Bertozzi, J. Heisenberg, S. Kowalski, X. Maruyama, C. P. Sargent, W. Turchinetz, C. F. Williamson, S. P. Fivozinsky, J. W. Lightbody, Jr., and S. Penner, Physical Review C, 7, pp.1396(1973).

29. H. Crannell, Physical Review, 148(3), pp.1107(1966).